AIAA JOURNAL
Vol. 30, No. 4, April 1992

Nonadiabatic and Three-Dimensional Effects in Compressible Turbulent Boundary Layers

Richard W. Barnwell*
NASA Langley Research Center, Hampton, Virginia 23665

A defect stream function formulation for nonadiabatic flow with small crossflow is developed. The first-integral property of this formulation provides for the removal of the streamline curvature term in the governing equation so that the form of the reduced equation for small crossflow is the same as that for two-dimensional flow. The combined law of the wall and wake is used in place of the no-slip boundary condition. A three-dimensional law-of-the-wall formulation is used to develop a closed-form solution for the crossflow angle near the wall. Analytic solutions for nonadiabatic, compressible, equilibrium flow with a Clauser outer-region eddy-viscosity model are obtained, and excellent agreement with experimental skin friction and velocity profile data for nonadiabatic, compressible flat-plate flow is achieved. An analytic solution for a linear inner-region eddy-viscosity model is also obtained; the wake function part of this solution is found to be inconsistent with the empirically established law of the wake. All comparisons with experiment are for two-dimensional equilibrium flow.

Introduction

RECENTLY, Barnwell and Wahls[1] developed an analytic solution for adiabatic, compressible, turbulent boundary-layer flows for which the profile of the deficit in velocity from the edge value normalized with the shear stress velocity is invariant to displacement in the streamwise direction in the outer region. Such flows, which are said to be in equilibrium, were originally studied experimentally by Clauser.[2,3] Flat-plate flow is an example. The equation that the analytic solution of Ref. 1 satisfies is an approximate form of the defect stream function equation for compressible boundary-layer flow. A principal advantage of the approximate equation is that it can be reduced to a second-order differential equation by means of a first integral. Wahls[4] and Wahls et al.[5] have shown with extensive numerical comparisons that solutions to the approximate form of the defect stream function equation agree remarkably well with solutions to the full-equation form. Wall boundary conditions are imposed by joining the analytic solution for the outer region to an empirical expression for the inner region composed of the laws of the wall and wake. A similar, simpler approach was used by Clauser[3] for incompressible flat-plate flow.

The application of the defect stream function formulation to the numerical solution of compressible flow is a generalization of a similar treatment for incompressible flow[6] that is based on the earlier analysis of Mellor and Gibson.[7] The principal difference in the methods of Refs. 6 and 7 is the manner in which the surface boundary conditions are imposed. Rather than use an empirical analytic expression in the inner region, Mellor and Gibson solved that region numerically using an inner-region eddy-viscosity model. The resulting solutions were difficult to implement and deviated from the experimentally observed laws of the wall and wake but agreed closely with experiment on skin friction. The method of Ref. 6 successfully overcame these disadvantages while maintaining the advantages.

The present paper presents results on three topics in turbulent boundary-layer analysis. These topics include the law of the wall for three-dimensional flow, the solution of nonadiabatic compressible flow, and the effectiveness of linear eddy-viscosity models in the inner region.

The Boussinesq approximation and a three-dimensional law-of-the-wall concept are used to derive a closed-form expression for the crossflow angle near the wall. In addition, the approximate second-order defect-layer governing equations for two dimensions and three dimensions with small crossflow are found to be the same.

The analytic solution of Ref. 1 for compressible turbulent equilibrium flow is extended to include nonadiabatic effects. Excellent agreement with experiment is demonstrated for several nonadiabatic, compressible, flat-plate flows.

The author has long been concerned about the redundancy and possible inconsistency of using both an eddy viscosity and the laws of the wall and wake in the inner region. An analytic solution is obtained for a linear inner-region eddy-viscosity model. This solution is inconsistent with the law of the wake and not completely compatible with the law of the wall.

Analysis

The zero-order defect equation for nonadiabatic compressible turbulent boundary-layer flow with small crossflow is derived, and the equilibrium form of this equation is solved in closed form. This solution pertains for all pressure gradients in the speed range from incompressible to supersonic and for small pressure gradients in the hypersonic range.

Physical Model

The continuity and tangential momentum equations for three-dimensional, compressible, turbulent boundary-layer flow are

$$\frac{\partial(\rho u)}{\partial x} + \frac{\partial(\rho v)}{\partial y} + \frac{\partial(\rho w)}{\partial z} = 0 \tag{1}$$

$$\rho u\frac{\partial u}{\partial x} + \rho v\frac{\partial u}{\partial y} + \rho w\frac{\partial u}{\partial z} - \rho\frac{uw}{R} - \rho\frac{w^2}{R}\frac{\partial R}{\partial x} + \frac{\partial p}{\partial x} = \frac{\partial}{\partial y}\left\{(\mu + \mu_t)\frac{\partial u}{\partial y}\right\} \tag{2}$$

Presented as Paper 91-0528 at the AIAA 29th Aerospace Sciences Meeting, Reno, NV, Jan. 7–10, 1991; received Feb. 5, 1991; revision received July 13, 1991; accepted for publication July 15, 1991.

*Chief Scientist. Asociate Fellow AIAA.

$$\rho u\frac{\partial w}{\partial x}+\rho v\frac{\partial w}{\partial y}+\rho w\frac{\partial w}{\partial z}+\rho\frac{u^2}{R}+\rho\frac{uw}{R}\frac{\partial R}{\partial x}+\frac{\partial p}{\partial z}$$

$$=\frac{\partial}{\partial y}\left\{(\mu+\mu_t)\frac{\partial w}{\partial y}\right\} \tag{3}$$

where the Boussinesq approximation has been used to model the turbulent shear stress terms. The x and z coordinates are the streamwise and stream-normal coordinates at the boundary-layer edge, R is the boundary-layer edge streamline radius of curvature, y the coordinate perpendicular to the surface, p and ρ the pressure and density, and μ and μ_t the viscosity and turbulent eddy viscosity. The velocity components in the x, y, and z directions are u, v, and w, respectively. Define the tangential velocity and tangential flow angle relative to the boundary-layer edge streamline as

$$U=[u^2+w^2]^{1/2},\qquad \theta=\tan^{-1}(w/u) \tag{4}$$

Equations that govern U and θ are derived from Eqs. (2-4) as

$$\cos\theta\,\rho U\frac{\partial U}{\partial x}+\rho v\frac{\partial U}{\partial y}+\sin\theta\,\rho U\frac{\partial U}{\partial z}+\cos\theta\frac{\partial p}{\partial x}+\sin\theta\frac{\partial p}{\partial z}$$

$$=\frac{\partial}{\partial y}\left\{(\mu+\mu_t)\frac{\partial U}{\partial y}\right\}-(\mu+\mu_t)U\left(\frac{\partial\theta}{\partial y}\right)^2 \tag{5}$$

$$\cos\theta\,\rho U^2\frac{\partial\theta}{\partial x}+\rho Uv\frac{\partial\theta}{\partial y}+\sin\theta\,\rho U^2\frac{\partial\theta}{\partial z}-\sin\theta\frac{\partial p}{\partial x}+\cos\theta\frac{\partial p}{\partial z}$$

$$+\rho\frac{U^2}{R}\left\{\cos\theta+\frac{\partial R}{\partial x}\sin\theta\right\}=2(\mu+\mu_t)\frac{\partial U}{\partial y}\frac{\partial\theta}{\partial y}$$

$$+U\frac{\partial}{\partial y}\left\{(\mu+\mu_t)\frac{\partial\theta}{\partial y}\right\} \tag{6}$$

In the defect part of the boundary layer, the viscosity μ is neglected and the eddy viscosity is modeled as

$$\mu_t=K\rho U_e\delta_i^* \tag{7}$$

where K can be a general nondimensional function of x, y, and z, and δ_i^* is the incompressible displacement thickness, which is sometimes called the velocity thickness. In this treatment, K will be given the value of the Clauser constant k in the outer part of the boundary layer.

The modified Crocco equation for nonadiabatic walls,

$$\frac{T_w}{T}=\frac{\rho}{\rho_w}=1-\frac{(T_{aw}-T_w)}{T}\frac{U}{U_e}+r\frac{(\gamma-1)}{2}\frac{U^2}{c^2} \tag{8}$$

is used as the energy equation, where T is the temperature, the subscript w designates properties of the wall, T_{aw} is the adiabatic wall temperature, γ the ratio of specific heats, c the local speed of sound, and r the recovery factor. In this treatment, the recovery factor will be evaluated as $r=Pr^{1/3}$, where Pr is the Prandtl number.

Three-Dimensional Law of the Wall

Several law-of-the-wall concepts for three-dimensional flow, which involve different tangential-velocity expressions, are discussed in Ref. 8. The concept of Prahlad[9] employs the expression U used here. The law-of-the-wall form of Eq. (5) is the limiting form as the velocity vanishes near the wall:

$$\cos\theta\frac{\partial p}{\partial x}+\sin\theta\frac{\partial p}{\partial z}=\frac{\partial}{\partial y}\left\{(\mu+\mu_t)\frac{\partial U}{\partial y}\right\}$$

The flow angle gradient $\partial\theta/\partial y$ does not appear. The pressure gradient is in the local streamwise direction, as in two-dimensional flow, and has only a higher-order effect. The principal term, the term on the right, is identical to that for two-dimensional flow and has the first integral

$$(\mu+\mu_t)\frac{\partial U}{\partial y}=\tau_w \tag{9}$$

where τ_w is the wall shear stress. All pressure-independent laws of the wall including those for three dimensions satisfy an equation of this form.

In general, three-dimensional law-of-the-wall behavior includes a variation in flow angle with distance from the wall at all distances from the wall. The limiting form of Eq. (6) for the tangential flow angle is

$$-\sin\theta\frac{\partial p}{\partial x}+\cos\theta\frac{\partial p}{\partial z}=2\,\tau_w\frac{\partial\theta}{\partial y}$$

The solution is

$$\tan\{\tfrac{1}{2}(\theta-\phi)\}=\tan\{\tfrac{1}{2}(\theta_w-\phi)\}\,e^{-p'y/2\tau_w}$$

where the pressure-gradient magnitude p' and the angle ϕ between the pressure gradient and boundary-layer edge streamline are defined as

$$p'=\left[\left(\frac{\partial p}{\partial x}\right)^2+\left(\frac{\partial p}{\partial z}\right)^2\right]^{1/2}$$

$$\phi=\tan^{-1}\left(\frac{\partial p}{\partial z}\Big/\frac{\partial p}{\partial x}\right)$$

This is an inner solution that pertains only near the wall. It cannot be used for large y where it indicates erroneously that θ approaches ϕ rather than zero asymptotically; this limitation occurs because the second-order derivative in the differential equation for θ is removed by the approximation process so that the outer boundary condition cannot be enforced. This solution predicts that the tangential velocity will continue to change direction all the way to the wall unless θ_w, the flow angle at the wall, and ϕ, the direction angle of the pressure gradient, are the same. In that case, the tangential velocity and the pressure gradient are aligned throughout the inner part of the boundary layer so that the flow angle does not change. These results may explain why some three-dimensional boundary layers appear to be two dimensional near the wall and others do not. Note that the assumption that the tangential velocity and shear stress vectors are aligned is implicit in the Boussinesq approximation.

Small Crossflow Approximation

For small crossflow, Eq. (5) becomes

$$\rho U\frac{\partial U}{\partial x}+\rho v\frac{\partial U}{\partial y}-\rho_e U_e\frac{\partial U_e}{\partial x}=\frac{\partial}{\partial y}\left\{(\mu+\mu_t)\frac{\partial U}{\partial y}\right\} \tag{10}$$

and Eq. (1) for mass conservation becomes

$$\frac{\partial(\rho U)}{\partial x}+\frac{\rho U}{R}\frac{\partial R}{\partial x}+\frac{\partial(\rho v)}{\partial y}=0 \tag{11}$$

where the subscript e designates properties at the boundary-layer edge. Cooke[10] first obtained these equations and noted that they are analogous to those for axisymmetric flow. In the present treatment, a first integral to the governing equation is obtained that eliminates explicit dependence on R and makes the small-crossflow, three-dimensional problem analogous to the two-dimensional problem.

Defect Stream Function Formulation

The defect formulation of Clauser[2] is modified to account for compressibility. The defect stream function $f[x,z,\eta(x,y,z)]$ is defined as

$$\frac{\partial f}{\partial \eta}=\frac{U-U_e}{u^*} \tag{12}$$

where

$$\eta=\frac{1}{\Delta}\int^{y}\frac{\rho}{\rho_e}\,\mathrm{d}y \tag{13}$$

The shear stress velocity u^* is

$$u^*=[\tau_w/\rho_w]^{1/2}$$

and the boundary-layer thickness parameter Δ is defined so that the profiles of the nondimensional defect velocity $(U_a-U)u^*$ vs η will be self-similar for equilibrium flow. The equation is

$$\Delta=\int_0^\infty \frac{U_e-U}{u^*}\frac{\rho}{\rho_e}\,\mathrm{d}y=\frac{U_e}{u^*}\delta_v^* \tag{14}$$

where the density-weighted velocity thickness δ_v^* is

$$\delta_v^*=\int_0^\infty \frac{\rho}{\rho_e}\left(1-\frac{U}{U_e}\right)\mathrm{d}y$$

The zero-order governing equation for f is obtained from Eq. (10) in the limit of small u^*/U_e. The derivatives of U are

$$\frac{\partial U}{\partial x}=\frac{\mathrm{d}U_e}{\mathrm{d}x}\left(1+\frac{u^*}{U_e}\frac{\partial f}{\partial \eta}\right)+U_e\frac{\partial}{\partial x}\left(\frac{u^*}{U_e}\frac{\partial f}{\partial \eta}\right)+u^*\frac{\partial^2 f}{\partial \eta^2}\frac{\partial \eta}{\partial x}$$

$$\frac{\partial U}{\partial y}=\frac{\rho}{\rho_e}\frac{u^*}{\Delta}\frac{\partial^2 f}{\partial \eta^2}$$

The normal mass flux is obtained from Eq. (11) as

$$\rho v=-\frac{1}{R}\frac{\mathrm{d}}{\mathrm{d}x}(\rho_e U_e R\Delta)\left(\eta+\frac{u^*}{U_e}f\right)-\rho_e U_e\Delta\frac{\partial}{\partial x}\left(\frac{u^*}{U_e}f\right)-\rho_e U_e\Delta\left(1+\frac{u^*}{U_e}\frac{\partial f}{\partial \eta}\right)\frac{\partial \eta}{\partial x}$$

It will be shown later that

$$\frac{\partial}{\partial x}\left(\frac{u^*}{U_e}\right)=\mathcal{O}\left(\left[\frac{u^*}{U_e}\right]^2\right)$$

so that this derivative can be neglected. The density ratio ρ_e/ρ is obtained from Eqs. (8) and (12) as

$$\frac{\rho_e}{\rho}=1-\left(\frac{T_{aw}+T_w}{T_e}-2\right)\frac{u^*}{U_e}\frac{\partial f}{\partial \eta}-\left(\frac{T_{aw}}{T_e}-1\right)\left(\frac{u^*}{U_e}\frac{\partial f}{\partial \eta}\right)^2 \tag{15}$$

To the lowest order, Eq. (10) is

$$\frac{\partial}{\partial \eta}\left\{\omega K\left(\frac{\rho}{\rho_e}\right)^2\frac{\partial^2 f}{\partial \eta^2}+\left(1+\frac{T_{aw}}{T_w}\right)\beta f-\frac{\partial f}{\partial s}-\left(1+\frac{U_e}{\dot U_e}\left[\frac{\dot\Delta}{\Delta}+\frac{\dot R}{R}+\frac{\dot\rho_e}{\rho_e}\right]\right)\beta\frac{\rho_w}{\rho_e}\left(\eta\frac{\partial f}{\partial \eta}-f\right)\right\}=0 \tag{16}$$

where

$$s=\int^x\frac{u^*}{U_e\Delta}\,\mathrm{d}x$$

The dot represents differentiation with respect to x, and the pressure-gradient parameter β and the ratio ω are defined as

$$\beta=\frac{\delta_v^*}{\tau_w}\frac{\mathrm{d}p}{\mathrm{d}x}$$

$$\omega=\frac{\delta_i^*}{\delta_v^*}$$

There are two surface boundary conditions and one far-field boundary condition. The shear stress surface boundary condition is obtained from Eqs. (7), (9), (12), and (13) as

$$\lim_{\eta\to 0}\ \omega K\left(\frac{\rho}{\rho_e}\right)^2\frac{\partial^2 f}{\partial \eta^2}=\frac{\rho_w}{\rho_e}$$

From the equation for the normal mass flux ρv, it is concluded that f vanishes at the surface:

$$f(s,0)=0$$

The far-field condition is obtained from Eqs. (12–14):

$$\Delta=-\Delta\int_0^\infty\frac{\partial f}{\partial \eta}\,\mathrm{d}\eta=\Delta[f(s,0)-f_\infty(s)]$$

It follows that

$$f_\infty(s)=-1$$

With these boundary conditions, Eq. (16) can be integrated across the boundary layer to obtain

$$1+\frac{U_e}{\dot U_e}\left(\frac{\dot\Delta}{\Delta}+\frac{\dot R}{R}+\frac{\dot\rho_e}{\rho_e}\right)=-\left(1+\frac{T_{aw}}{T_w}\right)\frac{\rho_e}{\rho_w}-\frac{1}{\beta}$$

Therefore, the first integral of Eq. (16) for arbitrary η is

$$\frac{\rho_e}{\rho_w}\frac{\partial f}{\partial s}=\omega K\frac{\rho_e}{\rho_w}\left(\frac{\rho}{\rho_e}\right)^2\frac{\partial^2 f}{\partial \eta^2}+\left(1+\left[1+\frac{T_{aw}}{T_w}\right]\frac{\rho_e}{\rho_w}\beta\right)\eta\frac{\partial f}{\partial \eta}-f-1 \tag{17}$$

This equation, which pertains for small crossflow, is identical to the two-dimensional version; the explicit streamline curvature effect was removed when the first integral was taken.

The strong dependence of the coefficients of Eq. (17) on the ratio ρ_e/ρ_w can be removed with the transformation

$$\hat{s} = \int^s \frac{\rho_w}{\rho_e}\,\mathrm{d}s, \qquad \hat{\eta} = \left[\frac{\rho_w}{\rho_e}\right]^{1/2} \eta$$

The resulting governing equation for f is

$$\frac{\partial f}{\partial \hat{s}} = \omega K \left(\frac{\rho}{\rho_e}\right)^2 \frac{\partial^2 f}{\partial \hat{\eta}^2} + (1 + 2\hat{\beta})\hat{\eta}\frac{\partial f}{\partial \hat{\eta}} - f - 1 \tag{18}$$

where

$$\hat{\beta} = \frac{\beta}{2r}\left\{1 + \frac{T_e}{T_w} + [1 - r]\left(1 - \frac{T_e}{T_{aw}} - \frac{T_{aw}}{T_e} - \frac{T_w}{T_e}\right)\right\}$$

The expressions for the ratio $\omega = \delta_i^*/\delta_v^*$ and the density ratio ρ_e/ρ can be simplified. Equation (15) can be written as

$$\frac{\rho_e}{\rho} = 1 - \epsilon\frac{\partial f}{\partial \hat{\eta}} - \nu^2\left(\frac{\partial f}{\partial \hat{\eta}}\right)^2 \tag{19}$$

where

$$\epsilon = \left(1 + \frac{T_{aw}}{T_w} - 2\frac{\rho_w}{\rho_e}\right)\frac{u^*}{U_e}\left[\frac{\rho_e}{\rho_w}\right]^{1/2}$$

$$\nu = \left[\frac{T_{aw}}{T_w} - \frac{\rho_w}{\rho_e}\right]^{1/2}\frac{u^*}{U_e} = \left[\frac{r(\gamma - 1)}{2}\right]^{1/2}\frac{u^*}{c_w}$$

The last term in Eq. (19) varies as $(u^*/U_e)^2$ and can be neglected. For edge Mach numbers from incompressible to supersonic, the parameter ϵ is of the order u^*/U_e so that ρ_e/ρ is approximately 1 and Eq. (18) for f is linear. However, because this parameter has the asymptotic form

$$\epsilon \sim \left(1 + \frac{T_{aw}}{T_w}\right)\left[\frac{r(\gamma - 1)}{2}\right]^{1/2}\frac{u^*}{U_e}M_e, \qquad M_e \gg 1$$

where M_e is the edge Mach number, it is not small for large values of M_e and cannot be neglected. The most general approximate form of Eq. (19) is

$$\frac{\rho_e}{\rho} = 1 - \epsilon\frac{\partial f}{\partial \hat{\eta}} \tag{20}$$

The corresponding approximate form for ω is

$$\omega = \frac{\delta_i^*}{\delta_v^*} = 1 + \epsilon\int_0^\infty \left(\frac{\partial f}{\partial \hat{\eta}}\right)^2 \mathrm{d}\hat{\eta} \tag{21}$$

Coles[11] used the parameter $M_\infty^2 C_f$, where M_∞ is the freestream Mach number and C_f is the skin-friction coefficient, to correlate compressible boundary-layer data. This parameter corresponds to ϵ^2.

Wahls[4] and Wahls et al.[5] have shown that numerical solutions to the nonlinear equilibrium form of the present equation and the equilibrium form of the exact equation are virtually the same for adiabatic flow. These results indicate that the present approximate equation, which is much simpler than the exact equation, is an effective governing equation for the flow.

An additional transformation is needed to obtain a governing equation that is linear in the hypersonic range. Note that, with Eq. (20), Eq. (18) can be written as

$$\frac{\partial f}{\partial \hat{s}} = \omega K \frac{\partial}{\partial \hat{\eta}}\left(\frac{\rho}{\rho_e}\frac{\partial f}{\partial \hat{\eta}}\right) + (1 + 2\hat{\beta})\hat{\eta}\frac{\partial f}{\partial \hat{\eta}} - f - 1 \tag{22}$$

The additional transformation is

$$\tilde{s} = \hat{s}, \qquad \tilde{\eta} = \int \frac{\rho_e}{\rho}\,\mathrm{d}\hat{\eta} = \hat{\eta} - \epsilon f$$

In these coordinates, Eqs. (20) and (21) are

$$\frac{\rho}{\rho_e} = 1 + \epsilon\frac{\partial f}{\partial \tilde{\eta}}$$

$$\omega = 1 + \epsilon\int_0^\infty \left(1 + \epsilon\frac{\partial f}{\partial \tilde{\eta}}\right)^{-1}\left(\frac{\partial f}{\partial \tilde{\eta}}\right)^2 \mathrm{d}\tilde{\eta}$$

and Eq. (22) for f becomes

$$\frac{\partial f}{\partial \tilde{s}} = \omega K\frac{\partial^2 f}{\partial \tilde{\eta}^2} + (1 + 2\hat{\beta})(\tilde{\eta} - \tilde{\eta}_w)\frac{\partial f}{\partial \tilde{\eta}} - f - 1 - \epsilon\tilde{\beta}f\frac{\partial f}{\partial \tilde{\eta}} \tag{23}$$

where

$$\tilde{\eta}_w = \epsilon/(1 + 2\hat{\beta})$$

$$\tilde{\beta} = \frac{\beta}{r}\left(1 + \frac{T_{aw}}{T_w}\right)\left\{\left(\frac{T_{aw}}{T_w} - 1\right)\frac{\rho_e}{\rho_w}r + 2[1 - r]\left(\frac{T_{aw}}{T_w} + \frac{T_e}{T_{aw}} - 2\right)\right\}\Big/\left(1 + \frac{T_{aw}}{T_w} - 2\frac{\rho_w}{\rho_e}\right)$$

This equation is linear if the inequality

$$\epsilon|\tilde{\beta}| \ll 1 \tag{24}$$

is satisfied. This inequality is satisfied for all pressure gradients in the incompressible to supersonic range and for small pressure gradients in the hypersonic range. The inequality is also satisfied for all adiabatic flows with a recovery factor of 1.

Equilibrium Outer Solution

Clauser[2,3] defined turbulent boundary layers with pressure and skin-friction forces that are proportional along streamlines to be in equilibrium and showed that the defect velocity profiles at different streamwise stations are self-similar. The defect stream function f has no streamwise variation for such flows so that the left side of Eq. (23) vanishes. Mathematically, this null value can occur only if the coefficients of the equation do not depend on streamwise location. It is assumed that the eddy-viscosity coefficient K is equal to the Clauser constant k in the defect part of the boundary layer. Thus, the boundary layer is in equilibrium if the pressure-gradient parameter $\tilde{\beta}$ is constant and inequality (24) is satisfied. Note that $\tilde{\eta}_w$ and ω are both effectively constant when the inequality is satisfied.

As Mellor and Gibson[7] discovered for the incompressible problem, the governing equation for compressible equilibrium flow is the confluent hypergeometric equation. With the independent and dependent variables

$$N = \frac{1+2\hat{\beta}}{\omega k}\frac{(\bar{\eta}-\bar{\eta}_w)^2}{2}, \qquad \hat{f} = (1+f)e^N$$

the linear equilibrium form of Eq. (23) is

$$N\frac{d^2\hat{f}}{dN^2} + (b-N)\frac{d\hat{f}}{dN} - a\hat{f} = 0 \tag{25}$$

where

$$a = \frac{1}{2}\left(1+\frac{1}{1+2\hat{\beta}}\right), \qquad b = \frac{1}{2}$$

The solution to Eq. (25) that satisfies the far-field boundary condition $\hat{f}_\infty = 0$ is

$$\hat{f} = C\left\{M(a,b,N) - \frac{a}{b}\frac{\Gamma(1+a-b)}{\Gamma(1+a)}N^{1-b}M(1+a-b,2-b,N)\right\}$$

where C is an arbitrary constant to be evaluated with an inner-boundary condition, and $M(a,b,N)$ is Kummer's function[12]:

$$M(a,b,N) = 1 + \frac{a}{b}N + \frac{a\,(a+1)}{b\,(b+1)}\frac{N^2}{2!} + \ldots$$

The first derivative of f is

$$\frac{df}{d\bar{\eta}} = -C\left\{\frac{a}{[(a-½)\omega k]^{½}}\frac{\Gamma(½+a)}{\Gamma(1+a)}M\left(a-\frac{1}{2},\frac{1}{2},N\right) - \frac{(\bar{\eta}-\bar{\eta}_w)}{\omega k}M\left(a,\frac{3}{2},N\right)\right\}e^{-N} \tag{26}$$

This derivative is expressed in terms of the gamma functions $\Gamma(½+a)$ and $\Gamma(1+a)$ because they both have values very near 1 for all unfavorable pressure gradients and because their ratio is evaluated easily for favorable pressure gradients.

Inner Empirical Formulation

The tangential velocity near the wall is obtained from the combined law of the wall and wake, which is written as

$$U = u^*\{g(y^+) + h(\bar{\eta})\} \tag{27}$$

where

$$y^+ = \frac{\rho_w u^* y}{\mu_w} = \frac{Re_{\delta^*}}{\omega}\left[\frac{\rho_e}{\rho_w}\right]^{½}\tilde{\eta}$$

$$\bar{\eta} = \frac{y}{\Delta} = \left[\frac{\rho_e}{\rho_w}\right]^{½}\tilde{\eta}$$

$$Re_{\delta^*} = \frac{\rho_w U_e \delta_i^*}{\mu_w}$$

The law of the wall is one of the most well-established empiricisms in fluid mechanics. Prandtl developed a turbulence model that, when substituted into the inner limit of the tangential momentum equation, produces the law of the wall. However, there is no comparable algebraic turbulence model that produces the law of the wake. In fact, the closed-form solution that can be obtained to the linear equilibrium form of Eq. (23) and a Prandtl-like eddy-viscosity model contains a wake component that differs from the accepted empirical expression in both sign and form.

Law of the Wall

Prandtl developed an eddy-viscosity model of the form

$$\mu_t = \rho\ell^2\frac{\partial u}{\partial y} = \rho U_e \delta_i^* K, \qquad \ell = \kappa y \tag{28}$$

where ℓ is the mixing length and κ is one of the von Karman constants. With this model, van Driest[13] solved the two-dimensional form of Eq. (9), ignoring the viscosity μ, for compressible, nonadiabatic flow with a recovery factor of 1. The van Driest wall function that accommodates an arbitrary recovery factor is

$$g(y^+) = \frac{1}{\nu}\left(\sin\left[\nu\left(\frac{1}{\kappa}\ell n\,y^+ + B\right)\right] + \frac{½[(T_{aw}/T_w)-1]}{[(T_{aw}/T_w)-(\rho_w/\rho_e)]^{½}}\left\{1-\cos\left[\nu\left(\frac{1}{\kappa}\ell n\,y^+ + B\right)\right]\right\}\right) \tag{29}$$

where B is the other von Karman constant. This expression is the outer limit of the inner solution for the tangential velocity.

Law of the Wake

In this treatment, it is required that the law of the wake be defined only in the inner part of the boundary layer. Consequently, the form of the law of the wake used here contains only one term:

$$h(\bar{\eta}) = \frac{6}{\kappa}W\bar{\eta}^2 \tag{30}$$

This form of the leading term is used in the empirical formulations of both Coles[14] and Moses.[15]

Wahls[4] shows that the coefficient W can be evaluated iteratively by curve fitting the values of $h = U/u^* - g$ and $\bar{\eta}^2$ at points near the wall but beyond the point where the inner and outer solutions are joined. This evaluation procedure for the law of the wake employs no empirical constants other than those already used for the law of the wall. Wahls also shows that the values for the W for adiabatic compressible flow can be correlated as

$$W(\hat{\beta}) = W_i(\hat{\beta})\left(\frac{\rho_w}{\rho_e}\right)^\alpha$$

$$\alpha = 2 - \exp\left\{-\frac{5}{4}(1+2\hat{\beta})^{½}\right\}$$

where W_i is obtained from the correlation of White[8] for incompressible equilibrium flow:

$$W_i(\beta) = \Pi\left(\frac{1+\Pi}{\kappa}\right)^2, \qquad \Pi = \frac{4}{5}\left(\frac{1}{2}+\beta\right)^{¾}$$

Joining of Solutions

The skin friction is determined by equating the inner and outer solutions for U at the point where the inner and outer eddy viscosities are equal. This differs from the more formal procedures of matching the inner limit of the outer solution to the outer limit of the inner solution asymptotically. However, both procedures involve patching the outer and inner eddy-viscosity models at the point where they are equal. Two inner-region eddy-viscosity models are studied: the Prandtl model and the simpler linear model. The solution associated with the Prandtl model is in best agreement with experiment.

Linear Inner Eddy-Viscosity Model

An analytic solution is obtained for compressible equilibrium flow. This solution is completely compatible with the law of the wall only for incompressible flow and is generally incompatible with the law of the wake.

The governing equation for equilibrium compressible flow with a linear eddy-viscosity model that satisfies inequality (24) is the confluent hypergeometric equation. The classic linear eddy-viscosity model for the inner region is

$$\mu_t = \rho u^* \kappa y$$

which corresponds to

$$K = \frac{\kappa}{\omega}\left[\frac{\rho_e}{\rho_w}\right]^{1/2}\tilde{\eta}, \qquad \tilde{\eta} \le \frac{\omega k}{\kappa}\left[\frac{\rho_w}{\rho_e}\right]^{1/2}$$

With the transformations

$$\tilde{f} = f + 1, \qquad n = -\tilde{n} = \frac{1+2\hat{\beta}}{\kappa}\left[\frac{\rho_w}{\rho_e}\right]^{1/2}\tilde{\eta}$$

the linear equilibrium form of Eq. (23) becomes

$$\tilde{n}\frac{d^2\tilde{f}}{d\tilde{n}^2} + (\tilde{b} - \tilde{n})\frac{d\tilde{f}}{d\tilde{n}} - \tilde{a}\tilde{f} = 0$$

where

$$\tilde{a} = -1 + \hat{a}, \qquad \hat{a} = \frac{2\hat{\beta}}{1+2\hat{\beta}}, \qquad \tilde{b} = -\frac{\epsilon}{\kappa}\left[\frac{\rho_w}{\rho_e}\right]^{1/2}$$

Table 1 Comparison of shear-stress velocity ratio with experiment for adiabatic flow

M_e	$\hat{\beta}$	Re_{δ^*}	u^*/U_e, analytical	u^*/U_e, experiment
0	1.888	20,230	0.0291	0.0319
0	7.531	30,692	0.0223	0.0231
1.724	0	4,719	0.0423	0.0414
2.578	0	5,295	0.0431	0.0426
4.544	0	902	0.0556	0.0544

Table 2 Comparison of shear-stress velocity ratio with experiment for nonadiabatic flat-plate flow

M_e	T_{aw}/T_w	Re_{δ^*}	u^*/U_e, analytical	u^*/U_e, experiment
4.63	1.00	28,040	0.0392	0.0412
4.69	1.37	23,881	0.0365	0.0376
4.78	1.89	19,040	0.0354	0.0359
4.92	5.41	47,377	0.0260	0.0278
4.88	5.54	38,270	0.0269	0.0285
11.5	2.26	936	0.0480	0.0498

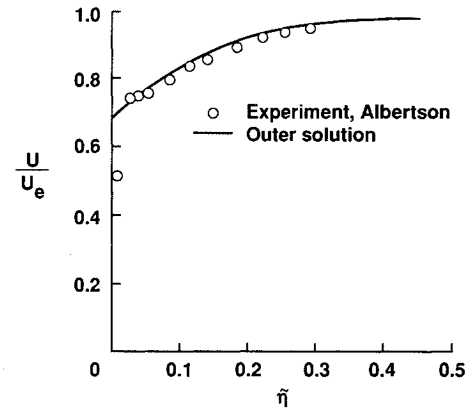

Fig. 1 Velocity profile for flat-plate air boundary layer with $M_e = 4.92$, $Re_{\delta^*} = 47{,}377$, $T_{aw}/T_w = 5.41$.

The pertinent solution is

$$\tilde{f} = n^{1-\tilde{b}} e^{-n}\left\{\frac{\sin \pi\tilde{b}}{\pi\tilde{b}}\Gamma(2-\hat{a})\,\Gamma(1+\tilde{b})\,U(2-\hat{a}, 2-\tilde{b}, n) + D\,M(2-\hat{a}, 2-\tilde{b}, n)\right\}$$

$$\frac{\partial f}{\partial\tilde{\eta}} = \frac{1+2\hat{\beta}}{\kappa}\left[\frac{\rho_w}{\rho_e}\right]^{1/2} n^{-\tilde{b}} e^{-n} \times \left\{-\frac{\sin \pi\tilde{b}}{\pi\tilde{b}}\Gamma(2-\hat{a})\,\Gamma(1+\tilde{b})\,U(1-\hat{a}, -\tilde{b}, n) + D(1-\tilde{b})\,M(1-\hat{a}, 1-\tilde{b}, n)\right\} \tag{31}$$

where the boundary condition $f(0) = 0$ has been applied and where the function $U(a, b, n)$ is a tabulated linear combination of two Kummer functions which contains the logarithm $\ln(n)$ if b is an integer (see Ref. 12). The constants C and D in Eqs. (26) and (31), respectively, are evaluated by equating the outer and inner expressions for f and $\partial f/\partial\eta$ at the point where the outer and inner eddy-viscosity models are equal.

Because the parameter $\tilde{b}$ is scaled by the ratio u^*/U_e for all Mach numbers and, hence, is always small, the quantities $1 - \tilde{b}$ and $2 - \tilde{b}$ are, in effect, integers, and the solution contains a logarithmic term. The solution for the tangential velocity U is

$$\frac{U - U_e}{u^*} = \frac{\partial f}{\partial\eta}$$

$$= \frac{1}{\kappa}\frac{\rho_w}{\rho}\left\{M(\hat{a}, 1, -n)[\ln n + (1+2\hat{\beta})D + \pi\cot\pi\hat{a}] - \pi\cot\pi\hat{a} + 2\gamma_o + \psi(1-\hat{a}) - \frac{1}{\Gamma(\hat{a})}\sum_{j=1}^{\infty}[2\psi(1+j) - \psi(\hat{a}+j)]\frac{\Gamma(\hat{a}+j)(-n)^j}{(j!)^2}\right\}$$

where γ_o is the Euler constant and the function $\psi(a)$ is the derivative of $\ln\Gamma(a)$ with respect to a. This solution agrees with that of Bogucz and Walker[16] for incompressible flat-plate flow.

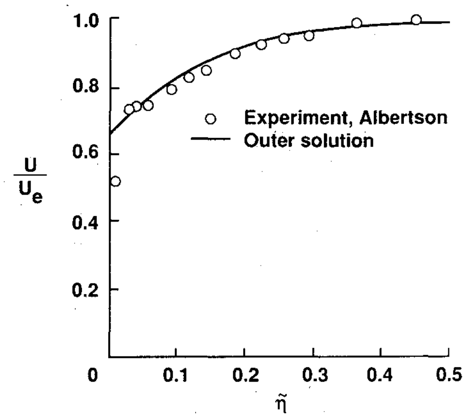

Fig. 2 Velocity profile for flat-plate air boundary layer with M_e = 4.88, Re_{δ^*} = 38,270, T_{aw}/T_w = 5.54.

The wake function for this solution is

$$h = \frac{1}{\kappa\Gamma(\hat{a})}\frac{\rho_w}{\rho}\sum_{j=1}^{\infty}[\pi\cot\pi\hat{a} + \ln n + (1+2\hat{\beta})D - 2\psi(1+j) + \psi(\hat{a}+j)]\frac{\Gamma(\hat{a}+j)(-n)^j}{(j!)^2}$$

For incompressible flat-plate flow, this function is

$$h = \frac{1}{\kappa}\sum_{j=1}^{\infty}\frac{(-\eta/\kappa)^j}{jj!}$$

These expressions fail to agree with the empirically observed function given by Eq. (30); the leading term is linear rather than quadratic in η and has the wrong sign. This failure indicates the need for an improvement of the linear inner-region eddy-viscosity model.

Prandtl Inner Eddy-Viscosity Model

The solution for this model has already been discussed in conjunction with the inner empirical formulation. The actual solution involves only the law of the wall; the law of the wake must be added empirically.

The equations for the point where the Clauser and Prandtl eddy viscosities are equal is obtained from Eqs. (7), (27-29), and (30) as

$$12W\tilde{\eta}_m^3 + \left\{\cos\left[\nu\left(\frac{1}{\kappa}\ln y_m^+ + B\right)\right] + \frac{\frac{1}{2}[T_{aw}/T_w - 1]}{[(T_{aw}/T_w) - (\rho_w/\rho_e)]^{1/2}}\sin\left[\nu\left(\frac{1}{\kappa}\ln y_m^+ + B\right)\right]\right\}\tilde{\eta}_m - \frac{\omega k}{\kappa} = 0$$

where the subscript m designates values at the patch point. This procedure is simpler than that used previously by the author[1,5,6] to determine the patch point by equating the outer and inner solutions for $\partial U/\partial y$. This simpler approach is used since it has been found that a 40% change in the patch point location results in no more than 1% change in the value of u^*/U_e.

The value of u^*/U_e is obtained by equating the outer and inner values of U at the patch point. The expression for the velocity is

$$U_m = U_e + u^*\left(\frac{\partial f}{\partial \eta}\right)_m = u^*\{g_m + h_m\}$$

which can be written as

$$\frac{u^*}{U_e} = \left\{g_m + h_m - \frac{\rho_e}{\rho_m}\left[\frac{\rho_w}{\rho_e}\right]^{1/2}\left(\frac{\partial f}{\partial\tilde{\eta}}\right)_m\right\}^{-1}$$

where the derivative of f is evaluated with Eq. (26) for equilibrium flow, and g_m and h_m are evaluated with Eqs. (29) and (30), respectively. This equation gives the skin-friction law.

In this paper, the coefficient C in Eq. (26) is evaluated at the patch point rather than with the surface boundary condition $f(0) = 0$ as in Ref. 1. The new procedure appears to be more accurate and is consistent with the numerical treatment of Refs. 4-6. With Eq. (12) and the definitions of η, $\hat{\eta}$, and $\tilde{\eta}$, the governing equation for the van Driest law of the wall is obtained from Eqs. (9) and (28) as

$$\left[\frac{\rho}{\rho_w}\right]^{1/2}\frac{\partial^2 f}{\partial\tilde{\eta}\partial\eta} = \frac{1}{\kappa\tilde{\eta}} = \left[\frac{\rho_e}{\rho}\right]^{3/2}\frac{\partial^2 f}{\partial\tilde{\eta}^2}$$

With this equation and integration by parts, an expression for f near the wall is derived as

$$f = \int_0^{\tilde{\eta}}\frac{\partial f}{\partial\tilde{\eta}}\mathrm{d}\tilde{\eta} = \tilde{\eta}\frac{\partial f}{\partial\tilde{\eta}} - \frac{1}{\kappa}\int_0^{\tilde{\eta}}\left[\frac{\rho}{\rho_e}\right]^{3/2}\mathrm{d}\tilde{\eta}$$

This equation is evaluated at $\tilde{\eta}_m$ with the outer solution using Eq. (26) and the comparable equation for f. The resulting expression for C is

$$C = \left\{1 - \frac{1}{\kappa}\int_0^{\tilde{\eta}_m}\left[\frac{\rho}{\rho_e}\right]^{3/2}\mathrm{d}\tilde{\eta}\right\}\left\{M(a, \tfrac{1}{2}, N_w) - \frac{a}{[(a-\frac{1}{2})\omega k]^{1/2}}\frac{\Gamma(\frac{1}{2}+a)}{\Gamma(1+a)}(\tilde{\eta}_m - \tilde{\eta}_w)M(a+\tfrac{1}{2}, \tfrac{3}{2}, N_m) + \tilde{\eta}_m\left[\frac{a}{[(a-\frac{1}{2})\omega k]^{1/2}}\frac{\Gamma(\frac{1}{2}+a)}{\Gamma(1+a)}M(a-\tfrac{1}{2}, \tfrac{1}{2}, N_m) - \frac{(\tilde{\eta}_m - \tilde{\eta}_w)}{\omega k}M(a, \tfrac{3}{2}, N_m)\right]\right\}^{-1} e^{N_m}$$

where

$$N_m = \frac{1+2\hat{\beta}}{\omega k}\frac{(\tilde{\eta}_m - \tilde{\eta}_w)^2}{2}$$

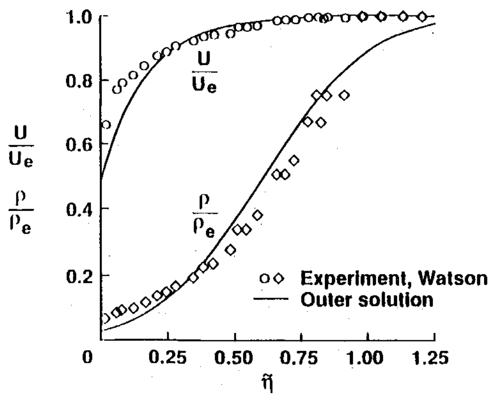

Fig. 3 Velocity and density profiles for flat-plate helium boundary layer with M_e = 11.5, Re_{δ^*} = 936, T_{aw}/T_w = 2.26.

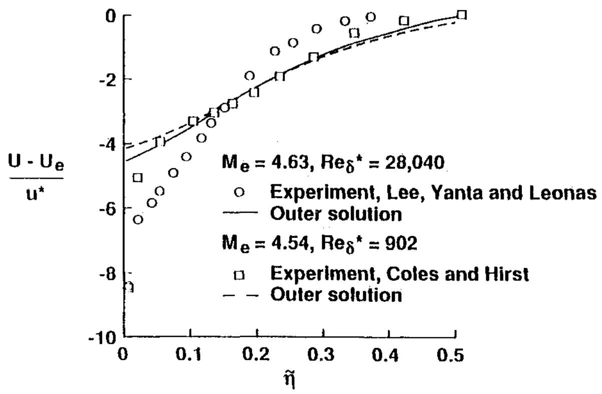

Fig. 4 Defect velocity profiles for flat-plate air boundary layers with $T_{aw}/T_w = 1.0$.

The streamwise gradient of u^*/U_e is

$$\frac{\partial}{\partial x}\left(\frac{u^*}{U_e}\right) = -\left(\frac{u^*}{U_e}\right)^2 \left\{\dot{g} + \dot{h} - \frac{\partial \dot{f}}{\partial \eta}\right\}_m$$

Thus, this derivative is, in fact, of second order in u^*/U_e so that its neglect earlier is justified.

Results

Both analytical and numerical results of the adiabatic form of the present method have been compared with experiment for a number of compressible and incompressible equilibrium turbulent flows.[1,4-6] The experimental values are obtained from the data compilations of Coles and Hirst[17] and Fernholz and Finley.[18] Some of the comparisons of shear-stress velocity to edge velocity ratios are given in Table 1. With one exception, the values for the ratio are within 4% of the relevant experimental values. This difference is at least comparable to experimental error.

Analytic results calculated with the nonadiabatic form of the present method have been compared with experiment for a number of compressible flat-plate flows. The experimental data that have been used have been measured by Lee et al.,[19] Albertson,[20] and Watson.[21] Analytic and experimental values for the shear-stress velocity to edge velocity ratio are compared in Table 2. The analytic values are within 7% of the relevant experimental values.

Analytic results for velocity profiles of nonadiabatic flows are compared with the experimental data of Albertson[20] in Figs. 1 and 2. The agreement between theory and experiment is good except near the wall where there is a small excursion in the experimental data.

Theoretical results for velocity and density profiles are compared with the results of Watson[21] for helium in Fig. 3. The density comparison shows that the present approximate Crocco equation is effective even for this rather severe case.

Substantial differences exist between the analytic velocity-profile results and the experimental data of Lee et al.[19] These differences are illustrated in Fig. 4 by a comparison of data for an adiabatic case from Ref. 19, adiabatic data for a comparable Mach number from Ref. 17, and the corresponding theoretical results. Both theoretical velocity profiles and the experimental profile of Ref. 17 agree closely and disagree sharply with the experimental profile of Ref. 19.

Conclusion

A closed-form solution for the flow angle variation near the wall of a three-dimensional turbulent boundary layer has been derived using a law-of-the-wall formulation.

The zero-order form of the defect steam function formulation for compressible nonadiabatic flow has been developed. This approximate formulation is shown to predict skin friction accurately for some two-dimensional adiabatic flows and nonadiabatic flat-plate flows.

With the present approximate formulation, the small-crossflow form of the three-dimensional boundary-layer equation is found to be identical to that for two-dimensional flow. This result occurs because the first integral property of the approximate formulation removes the explicit dependence on streamline curvature.

References

[1]Barnwell, R. W., and Wahls, R. A., "A Skin Friction Law for Compressible Turbulent Flow," *AIAA Journal,* Vol. 29, No. 3, 1991, pp. 380–386.

[2]Clauser, F. H., "Turbulent Boundary Layers in Adverse Pressure Gradients," *Journal of the Aeronautical Sciences,* Vol. 21, No. 2, 1954, pp. 91–108.

[3]Clauser, F. H., "The Turbulent Boundary Layer," *Advances in Applied Mechanics,* Vol. 4, Academic, New York, 1956, pp. 1–51.

[4]Wahls, R. A., "Development of a Defect Stream Function, Law of the Wall/Wake Method for Compressible Turbulent Boundary Layers," Ph.D. Dissertation, North Carolina State Univ., Raleigh, NC, 1989; also, NASA CR 4286, March 1990.

[5]Wahls, R. A., Barnwell, R. W., and DeJarnette, F. R., "A Defect Stream Function, Law of the Wall/Wake Method for Compressible Turbulent Boundary Layers," *AIAA Journal,* Vol. 28, No. 8, 1990, pp. 1432–1439.

[6]Barnwell, R. W., Wahls, R. A., and DeJarnette, F. R., "A Defect Stream Function, Law of the Wall/Wake Method for Turbulent Boundary Layers," *AIAA Journal,* Vol. 27, No. 12, 1989, pp. 1707–1713.

[7]Mellor, G. L., and Gibson, D. H., "Equilibrium Turbulent Boundary Layers," *Journal of Fluid Mechanics,* Vol. 24, Pt. 2, 1966, pp. 225–253.

[8]White, F. R., *Viscous Fluid Flow,* McGraw-Hill, New York, 1974.

[9]Prahlad, T. S., "Wall Similarity in Three-Dimensional Turbulent Boundary Layers," *AIAA Journal,* Vol. 6, No. 9, 1968, pp. 1772–1774.

[10]Cooke, J. C., "An Axially Symmetric Analogue for General Three-Dimensional Boundary Layers," Aeronautical Research Council, R&M 3200, London, June 1959.

[11]Coles, D. F., "The Turbulent Boundary Layer in a Compressible Fluid," Rand Corp., R-403-PR, Santa Monica, CA, Sept. 1962.

[12]Abramowitz, M., and Stegun, I. A. (eds.), *Handbook of Mathematical Functions with Formulas, Graphs, and Mathematical Tables,* Wiley, New York, 1964, pp. 504–515.

[13]Van Driest, E. R., "Turbulent Boundary Layer in Compressible Fluids," *Journal of the Aeronautical Sciences,* Vol. 18, No. 3, 1951, pp. 145–160, 216.

[14]Coles, D. F., "The Law of the Wake in the Turbulent Boundary Layer," *Journal of the Fluid Mechanics,* Vol. 1, Pt. 2, 1956, pp. 191–226.

[15]Moses, H. L., "The Behavior of Turbulent Boundary Layers in Adverse Pressure Gradients," Gas Turbine Lab., Massachusetts Inst. of Technology, Cambridge, MA, Rept. 73, Jan. 1964.

[16]Bogucz, E. A., and Walker, J. D. A., "Analysis and Prediction of the Turbulent Near Wake at a Sharp Trailing Edge," AIAA Paper 87-0483, Jan. 1987.

[17]Coles, D. F., and Hirst, E. A., *Proceedings of the Computation of Turbulent Boundary Layers,* Vol. II, Stanford Univ., Stanford, CA, 1968.

[18]Fernholz, H. H., and Finley, P. J., "A Critical Compilation of Compressible Turbulent Boundary Layer Data," AGARDograph 223, June 1977.

[19]Lee, R. E., Yanta, W. J., and Leonas, A. C., "Velocity Profile, Skin Friction Balance and Heat-Transfer Measurements of the Turbulent Boundary Layer at Mach 5 and Zero Pressure Gradient," U.S. Naval Ordnance Lab., TR-69-106, White Oak, MD, June 1969.

[20]Albertson, C. W., "Evaluation of Equilibrium Turbulence for a Hypersonic Boundary Layer at Nonadiabatic Wall Conditions," M.S. Thesis, Old Dominion Univ., Norfolk, VA, July 1989; also, NASA TM 101663, Nov. 1989.

[21]Watson, R. D., "Wall Cooling Effects on Hypersonic Transitional/Turbulent Boundary Layers at High Reynolds Numbers," *AIAA Journal,* Vol. 15, No. 10, 1977, pp. 1455–1461.